Gaussian-weighted parton quasi-distribution (Lattice Parton Physics Project ($\rm~~\bf{LP^3}$))

Tomomi Ishikawa, LuChang Jin, Huey-Wen Lin, Andreas Schäfer, Yi-Bo Yang, Jian-Hui Zhang and Yong Zhao

Gaussian-weighted parton quasi-distribution (Lattice Parton Physics Project (LP³))

Tomomi Ishikawa[1], LuChang Jin[2], Huey-Wen Lin[3,4], Andreas Schäfer[5],
Yi-Bo Yang[3], Jian-Hui Zhang[5*], and Yong Zhao[6]

[1]*T. D. Lee Institute, Shanghai Jiao Tong University, Shanghai 200240, China;*
[2]*Physics Department, Brookhaven National Laboratory, Upton, New York 11973, USA;*
[3]*Department of Physics and Astronomy, Michigan State University, East Lansing 48824, USA;*
[4]*Department of Computational Mathematics, Michigan State University, East Lansing 48824, USA;*
[5]*Institut für Theoretische Physik, Universität Regensburg, Regensburg D-93040, Germany;*
[6]*Center for Theoretical Physics, Massachusetts Institute of Technology, Cambridge 02139, USA*

Recent years have witnessed rapid progress in calculating parton distribution functions (PDFs), rather than just their moments, from lattice QCD [1-9]. The most remarkable aspect of such calculations is that one can connect appropriately chosen Euclidean correlation functions calculable on the lattice to PDFs through a perturbative matching relation. This can be understood in the framework of the large-momentum effective theory (LaMET) [10, 11]. According to LaMET, one can construct appropriate quasi-PDFs which are time-independent matrix elements defined at finite hadron momentum, and approach the PDFs in the infinite momentum limit. The PDFs can be extracted from lattice calculations of quasi-PDFs through a perturbative matching, up to power corrections suppressed by the hadron momentum. It is worthwhile to stress that the choice of quasi-PDFs is not unique; any construction is allowed as long as it approaches the PDFs in the infinite momentum limit and is practically calculable. This provides a flexibility to optimize the PDF results by choosing a suitable quasi-PDF that is best suited for lattice simulations.

The LaMET approach has been applied to compute the nucleon unpolarized, helicity and transversity PDFs [3, 5-8], as well as the pion distribution amplitude (DA) [12]. A first lattice PDF calculation at physical pion mass has also recently become available [13] (see also ref. [9]). In addition to LaMET, there also exist other proposals to use similar matrix elements or current-current correlators at spacelike separation to compute PDFs, meson DAs, etc. [4, 14-20].

The definition of quasi-PDFs in LaMET involves a spacelike Wilson line, which gives rise to linear divergences that have to be nonperturbatively renormalized. As shown in refs. [21-26], the renormalization of such linear divergences takes an exponential form that enhances the long-range correlations, and thereby significantly increases the uncertainties of the result [8]. A large value of the product of the hadron momentum and the length of the Wilson line, or the Ioffe-time, zp_z, is responsible for the small-x behavior of the PDF when Fourier transformed to momentum space. Given the small lattice hadron momentum used in current lattice calculations, the extracted PDF can not be trusted in the $x \lesssim 0.3$ region. In addition, since the matching is done perturbatively, using long distance input to reach large zp_z is also not justified, i.e. it introduces large systematic uncertainties. In, e.g. ref. [14] such contributions are suppressed by

*Corresponding author (email: jianhui.zhang@ur.de)

construction, forcing PDFs to vanish for Bjorken $x > 1$. In the LaMET approach we chose not to do so to be able to use the obtained large Bjorken x behavior as handle to estimate systematic uncertainties. The latter is needed if such results are used in global PDF analysis as in ref. [27]. Unless p_z can be made large enough to make the systematic errors small, lattice-PDFs will carry only very little weight in such fits. In ref. [13] two filtering techniques were thus used to estimate how large a p_z has to be reached to obtain reliable PDFs in the LaMET approach, where they also account for the truncation of the long-range correlations. To estimate the systematics introduced by the filter function, the authors of ref. [13] proposed to study the parameter setup done in actual lattice calculations using a known PDF input transformed to coordinate space and then back to x-space. This allows a very rough estimation of the systematics due to the Fourier transformation, the smallness of the hadron momentum and the lattice finite volume.

Here we propose a more systematic way to achieve the same effect. Just as there are many lattice fermion actions which lead to the same continuum Dirac fermion action, there are also a vast number of quasi-PDF constructions on the lattice which can reach the true lightcone PDF after the proper matching. We choose to revise Ji's quasi-PDFs definition by including a Gaussian weighting factor that suppresses long-range correlations and removes the unphysical oscillatory behavior. This construction only introduces a single parameter that we can control systematically with a known asymptotic large-momentum limit. Furthermore, all the perturbative matching results already done for the original quasi-PDF can be straightforwardly converted to those with the revised quasi-PDFs. As a demonstration, we show the impact of the Gaussian weighting on the isovector unpolarized quark PDF result presented in ref. [8].

Let us consider the definition of the quasi-PDF, taking the unpolarized quark quasi-PDF as an example. The discussion below applies equally well to other quark or gluon quasi-PDFs, meson quasi-DAs, etc. The unpolarized quark quasi-PDF is defined as:

$$\tilde{q}(x, \Lambda, p_z) = \int \frac{\mathrm{d}z}{4\pi} \mathrm{e}^{\mathrm{i}x p_z z} \langle p | \overline{\psi}(0, 0_\perp, z) \gamma^z L(z, 0) \psi(0) | p \rangle , \quad (1)$$

where the quark fields are separated along the spatial z-direction, $L(z, 0)$ is the Wilson-line gauge link inserted to ensure gauge invariance, $p_\mu = (p_0, 0, 0, p_z)$ is the nucleon momentum, and Λ denotes the UV cutoff or renormalization scale in an appropriate scheme such as the RI/MOM scheme used in refs. [8, 28].

Ref. [1] showed that the above quark quasi-PDF approaches the normal quark PDF in the infinite-momentum limit $p_z \to \infty$. It is worthwhile to point out that, although the z-integration in eq. (1) goes over non-perturbative large distances, for a large p_z the effective integration range shrinks

to small distances $z \sim 1/p_z$. In other words, the large p_z limit ensures the smallness of higher-twist corrections as well as perturbative corrections. In contrast, in the pseudo-distribution this is achieved by explicitly keeping z^2 small. Nevertheless, a large momentum is still required to probe information on higher moments. Therefore, the quasi- and pseudo-distribution approaches are actually equivalent.

In the following we will focus on the quasi-PDF and consider our revised definition for it. As mentioned earlier, any quark quasi-PDF that becomes the normal PDF in the limit $p_z \to \infty$ and is practically calculable offers an equally good candidate for lattice simulations. We consider the following definition with a Gaussian weighting factor

$$\tilde{q}_{\mathrm{GW}}(x, \Lambda, p_z)$$
$$= \int \frac{\mathrm{d}z}{4\pi} \mathrm{e}^{\mathrm{i}x p_z z - z^2/l^2} \langle p | \overline{\psi}(0, 0_\perp, z) \gamma^z L(z, 0) \psi(0) | p \rangle , \quad (2)$$

where l denotes a length scale. The above definition is related to the original one in eq. (1) by

$$\tilde{q}_{\mathrm{GW}}(x, \Lambda, p_z) = \int \frac{\mathrm{d}z}{4\pi} \mathrm{e}^{\mathrm{i}x p_z z} \left[2p_z \int \mathrm{d}y \, \mathrm{e}^{-\mathrm{i}y p_z z} \tilde{q}(y, \Lambda, p_z) \right]$$
$$\times \int \mathrm{d}t \frac{l p_z}{2\sqrt{\pi}} \mathrm{e}^{-\frac{t^2 l^2 p_z^2}{4}} \mathrm{e}^{-\mathrm{i}t p_z z}$$
$$= \int \mathrm{d}y \, \tilde{q}(y, \Lambda, p_z) \left[\frac{l p_z}{2\sqrt{\pi}} \mathrm{e}^{-\frac{l^2(x-y)^2 p_z^2}{4}} \right] . \quad (3)$$

In the limit $l p_z \gg 1$, the term in the square bracket yields a δ-function $\delta(x - y)$ and $\tilde{q}_{\mathrm{GW}}$ becomes $\tilde{q}$. For a relatively large $l p_z$, $\tilde{q}_{\mathrm{GW}}$ differs from $\tilde{q}$ only by power corrections suppressed by $1/(l p_z)^2$. Therefore, $\tilde{q}_{\mathrm{GW}}(x)$ is an equally good candidate for the quasi-PDF. In practice, the weighting parameter l can be tuned to optimize the PDF result extracted from lattice simulations, provided that the additional errors introduced by the weighting are under control.

In realistic lattice simulations, one can only have a finite lattice size and nucleon momentum. As a consequence, the z-integration in eq. (1) is always truncated, which then leads to an unphysical oscillation in $\tilde{q}$ obscuring the physical information embedded in it. This has been seen in the result of ref. [8]. As we will see below, eq. (2) has the advantage that, with an appropriate choice of the weighting parameter, the unphysical oscillation can be removed while the physical result remains unchanged in the moderate-to-large Bjorken x region. The price one has to pay is that the result in the small Bjorken x region is changed by the weighting. This is the most difficult region for lattice simulations and can not be trusted anyway at the current stage.

Some general remarks on the choice of weighting parameter follow. On one hand, in order that power corrections of $O(1/(l p_z)^2)$ can be safely neglected, one needs $l p_z \gg 1$. On the other hand, for a given p_z, z^2/l^2 shall not be too small for large z in order to have a suppression of the long-range

correlations. To find an optimal choice of l, let us take the CJ15 PDF [29] as an example. For simplicity, we use the central value only. We first Fourier transform the CJ15 PDF to coordinate space, then implement the Gaussian weighting in a truncated region, and transform back to momentum space. The Gaussian weighting is chosen to be in the form of e^{-cz^2/a^2} with a the lattice spacing and $c = a^2/l^2$. The results are shown in Figure 1. The green curves correspond to the Fourier transform of a truncated coordinate-space matrix element (with $ap_z = 2\pi/64\{6, 12, 24\}$ and $|z|/a \leq 32$ for Figure 1(a)-(c), and $ap_z = 2\pi/64 \times 24$ with $|z|/a \leq \{8, 16, 32\}$ for Figure 1(d)-(f)) generated from the CJ15 PDF data. A truncation like this is unavoidable in a realistic lattice simulation, and leads to an oscillation around the original CJ15 curve. As can be seen from the figure, adding a weighting factor indeed improves the oscillatory behavior. For a relatively large p_z in Figure 1(d)-(f), there exists a wide range of choices for c that removes the unphysical oscillation while retaining the original physical distribution at moderate to large x. This requires $|z|p_z$ to reach at least ~ 20 (estimated from Figure 1(d) with $z_{max} p_z = 32a \times 12\pi/(64a) \sim 20$). Moreover, the weighted distribution in the moderate-to-large x region remains essentially unchanged from top to bottom in Figure 1(d)-(f), indicating that information from large z is not important for constructing the PDF in that region. Of course, the distribution in small-x region changes significantly since it is determined by long-range correlations. Figure 1(a)-(c) shows that the larger momentum one has, the larger regions of the original curve one can recover from the weighted distribution and the less sensitivity to c one has at moderate to large x. In general, it is optimal to choose l in the perturbative range, in order to keep control of non-perturbative contributions. If we have $a = 0.05\,\text{fm}$, then for $c = 0.05$ we have $l \sim 1\,\text{GeV}^{-1}$, the weighted curve still deviates from the original curve at moderate to large x in Figure 1(b), while it essentially coincides with the original curve in the same region in Figure 1(c), which has twice the hadron momentum. This indicates that a larger momentum is important to achieve a suppression of unphysical oscillation without changing physics at moderate to large x.

The above example indeed gives some hint on the appropriate choice of c. In the following, we apply the Gaussian weighting to the lattice data presented in ref. [8], based on the above observation. Figure 2 shows the bare and renormalized matrix elements for nucleon momentum $p^z = 6\pi/L$ with $L \approx 3$ fm, together with the Gaussian weighted renormalized matrix elements. As an illustration, we show in Figure 2 the Gaussian weighted results for $c = 0.01, 0.02, 0.05$, respectively. One can clearly see a suppression of long-range correlations after including the Gaussian weighting factor.

From eq. (3), it is straightforward to write down the matching for $\tilde{q}_{GW}$, which is related to the matching for $\tilde{q}$ as following:
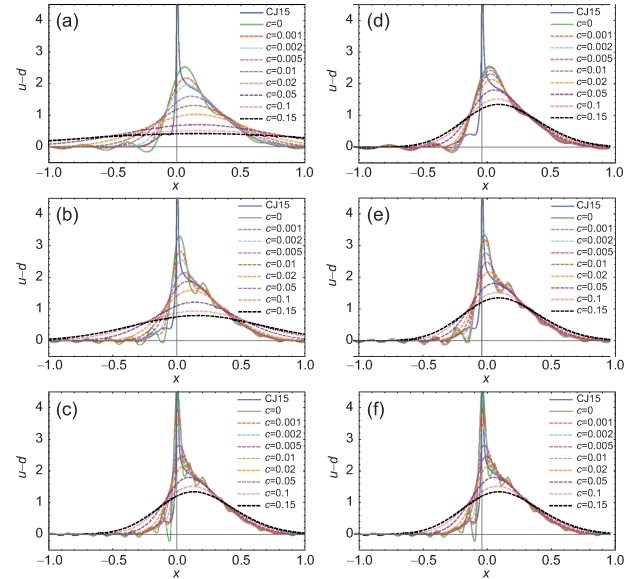

Figure 1 (Color online) CJ15 PDF with different Gaussian weighting. The blue curve is the original PDF, "$c=0$" denotes the Fourier transform result of a truncated coordinate space matrix element generated from CJ15 data without weighting. The dashed curves correspond to different Gaussian weighting factors. The plots correspond to $ap^z = \frac{2\pi}{64}\{6, 12, 24\}$ with $|z_{max}|/a = 32$ ((a)-(c)) and $ap^z = \frac{2\pi}{64} \times 24$ with $|z_{max}|/a = \{8, 16, 32\}$ ((d)-(f)), respectively.
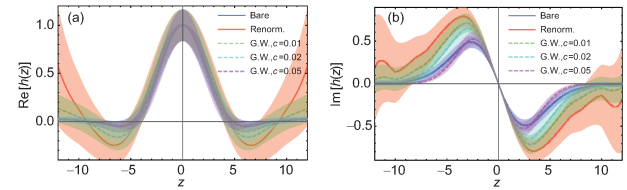

Figure 2 (Color online) Impact of the Gaussian weighting factor on lattice matrix elements. (a) The real part; (b) the imaginary part of the matrix elements.

$$\tilde{q}_{GW}(x, \Lambda, p^z)$$
$$= \int_{-1}^{1} \frac{du}{|u|} \int dy\, Z\left(\frac{y}{u}, \frac{\Lambda}{up^z}, \frac{\mu}{up^z}\right) q(u, \mu) \left[\frac{lp^z}{2\sqrt{\pi}} e^{-\frac{(x-y)^2 l^2 p_z^2}{4}}\right]$$
$$+ O(\Lambda_{QCD}^2/p_z^2, M^2/p_z^2, 1/(lp^z)^2),$$
$$= \int_{-1}^{1} \frac{du}{|u|} Z\left(\frac{x}{u}, \frac{\Lambda}{up^z}, \frac{\mu}{up^z}\right) q(u, \mu)$$
$$+ O(\Lambda_{QCD}^2/p_z^2, M^2/p_z^2, 1/(lp^z)^2), \tag{4}$$

where the power corrections $O(\Lambda_{QCD}^2/p_z^2, M^2/p_z^2, 1/(lp^z)^2)$ in the first line are related to those of the original quasi-distribution by eq. (3), while in the second line we move the additional $O(1/(lp^z)^2)$ power correction from introducing the weighting to the second term. The extra $O(1/(lp^z)^2)$ power correction introduced by Gaussian weighting is similar to that introduced by the gradient flow in ref. [30], where one needs a non-zero flow time τ to ensure a finite continuum limit of the quasi-PDF, but also needs to keep τ small to suppress the extra $O(\sqrt{\tau}\Lambda_{QCD})$ corrections. It is therefore important to find a window for τ so that both can be achieved. In our case, we need to keep a non-zero $1/l$ to suppress long-range
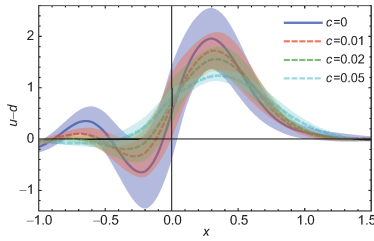
Figure 3 (Color online) Impact of the Gaussian weighting factor on momentum space distribution.

correlations, on the other hand, $1/l$ shall not be too large so that the extra $O(1/(lp^z)^2)$ corrections are still under control.

In Figure 3, we show the impact of the Gaussian weighting on momentum-space distribution obtained in ref. [8]. To estimate the extra $O(1/(lp_z)^2)$ errors in eq. (4), we did a simple extrapolation to infinite momentum as in ref. [8], i.e., and we have assumed a simple functional form of the power corrections like $a(x) + b(x)/p_z^2$ and used the results at different p_z to determine the leading term $a(x)$. As can be seen from the plot, including the Gaussian weighting reduces the oscillation in the negative x region observed in ref. [8], which was due to a cutoff in long-range correlations. Moreover, the Gaussian weighting introduces a significant change for the distribution in the small-x region, but only a slight change at moderate to large x, reflecting the large systematic error in the small-x region for current lattice setups. The maximum zp_z in this study is obviously not large enough, but the results provide a quantitative estimate on which x region the PDF extracted from current lattice data can be trusted.

In this paper, we have considered a revised quasi-distribution by including a Gaussian weighting factor, which naturally suppresses the long-range correlation, even after renormalization of the Wilson line. It improves the oscillatory behavior of the isovector unpolarized quark PDF observed in ref. [8]. The advantage of the revised quasi-PDF considered in this paper is that the matching function and power corrections can be straightforwardly obtained from the known ones for the standard quasi-PDF. A straightforward generalization of the Gaussian weighting presented in this paper is to use a superposition of different Gaussian factors or a p_z-dependent weighting parameter c, which can also be easily implemented. It is highly probable that more effective modifications of quasi-PDFs can be found, which will, however, usually require a recalculation of the matching function and power corrections.

1   X. Ji, Phys. Rev. Lett. **110**, 262002 (2013), arXiv: 1305.1539.
2   X. Xiong, X. Ji, J. H. Zhang, and Y. Zhao, Phys. Rev. D **90**, 014051 (2014), arXiv: 1310.7471.
3   H. W. Lin, J. W. Chen, S. D. Cohen, and X. Ji, Phys. Rev. D **91**, 054510 (2015), arXiv: 1402.1462.
4   Y. Q. Ma, and J. W. Qiu, Phys. Rev. Lett. **120**, 022003 (2018), arXiv: 1709.03018.
5   C. Alexandrou, K. Cichy, V. Drach, E. Garcia-Ramos, K. Hadjiyiannakou, K. Jansen, F. Steffens, and C. Wiese, Phys. Rev. D **92**, 014502 (2015), arXiv: 1504.07455.
6   J. W. Chen, S. D. Cohen, X. Ji, H. W. Lin, and J. H. Zhang, Nucl. Phys. B **911**, 246 (2016), arXiv: 1603.06664.
7   C. Alexandrou, K. Cichy, M. Constantinou, K. Hadjiyiannakou, K. Jansen, F. Steffens, and C. Wiese, Phys. Rev. D **96**, 014513 (2017), arXiv: 1610.03689.
8   J. W. Chen, T. Ishikawa, L. Jin, H. W. Lin, Y. B. Yang, J. H. Zhang, and Y. Zhao, Phys. Rev. D **97**, 014505 (2018), arXiv: 1706.01295.
9   C. Alexandrou, S. Bacchio, K. Cichy, M. Constantinou, K. Hadjiyiannakou, K. Jansen, G. Koutsou, A. Scapellato, and F. Steffens, EPJ Web Conf. **175**, 14008 (2018), arXiv: 1710.06408.
10   X. D. Ji, Sci. China-Phys. Mech. Astron. **57**, 1407 (2014), arXiv: 1404.6680.
11   X. Ji, J. H. Zhang, and Y. Zhao, Nucl. Phys. B **924**, 366 (2017), arXiv: 1706.07416.
12   J. H. Zhang, J. W. Chen, X. Ji, L. Jin, and H. W. Lin, Phys. Rev. D **95**, 094514 (2017), arXiv: 1702.00008.
13   H. W. Lin, J. W. Chen, T. Ishikawa, and J. H. Zhang, Phys. Rev. D **98**, 054504 (2018), arXiv: 1708.05301.
14   A. V. Radyushkin, Phys. Rev. D **96**, 034025 (2017).
15   Z. Davoudi, and M. J. Savage, Phys. Rev. D **86**, 054505 (2012), arXiv: 1204.4146.
16   W. Detmold, and C. J. D. Lin, Phys. Rev. D **73**, 014501 (2006).
17   K. F. Liu, and S. J. Dong, Phys. Rev. Lett. **72**, 1790 (1994).
18   J. Liang, K. F. Liu, and Y. B. Yang, EPJ Web Conf. **175**, 14014 (2018), arXiv: 1710.11145.
19   V. M. Braun, and D. Müller, Eur. Phys. J. C **55**, 349 (2008), arXiv: 0709.1348.
20   G. S. Bali, V. M. Braun, B. Gläßle, M. Göckeler, M. Gruber, F. Hutzler, P. Korcyl, B. Lang, A. Schäfer, P. Wein, and J. H. Zhang, Eur. Phys. J. C **78**, 217 (2018), arXiv: 1709.04325.
21   H. Dorn, Fortschr. Phys. **34**, 11 (1986).
22   T. Ishikawa, Y. Q. Ma, J. W. Qiu, and S. Yoshida, arXiv: 1609.02018.
23   J. W. Chen, X. Ji, and J. H. Zhang, Nucl. Phys. B **915**, 1 (2017), arXiv: 1609.08102.
24   X. Ji, J. H. Zhang, and Y. Zhao, Phys. Rev. Lett. **120**, 112001 (2018), arXiv: 1706.08962.
25   T. Ishikawa, Y. Q. Ma, J. W. Qiu, and S. Yoshida, Phys. Rev. D **96**, 094019 (2017), arXiv: 1707.03107.
26   J. Green, K. Jansen, and F. Steffens, Phys. Rev. Lett. **121**, 022004 (2018), arXiv: 1707.07152.
27   E. R. Nocera, H. W. Lin, F. Olness, K. Orginos, and J. Rojo, arXiv: 1709.01511.
28   I. W. Stewart, and Y. Zhao, Phys. Rev. D **97**, 054512 (2018), arXiv: 1709.04933.
29   A. Accardi, L. T. Brady, W. Melnitchouk, J. F. Owens, and N. Sato, Phys. Rev. D **93**, 114017 (2016), arXiv: 1602.03154.
30   C. Monahan, and K. Orginos, J. High Energ. Phys. **2017(3)**, 116 (2017), arXiv: 1612.01584.